Ship Azimuth Velocity Estimation in TerraSAR-X data based on Minimum-Entropy Criterion

Dongyang Ao, Beijing Institute of Technology, aodongyang@qq.com, China
Mihai Datcu, Germany Aerospace Center (DLR), Mihai.Datcu@dlr.de, Germany

Abstract

This paper proposed a new method to estimate the ship azimuth velocity in TerraSAR-X data based on the minimum-entropy criterion. The moving targets in synthetic aperture radar images are blurred because of the mismatch of the desired signal of stationary targets. Applying the image entropy, a simple parameter to evaluate the extent of the defocusing, the azimuth velocity can be recovered through searching the minima of the entropy curves. The signal models of moving targets are analyzed and their behaviors in SAR images are deduced in this paper. Experiment results show that our method for estimating ship azimuthal velocities in TerraSAR-X data has high precision and is robust.

1 Introduction

Detecting moving target is an important task in monitoring traffic both in ground and sea. There are many platforms to monitor the traffic information, such as optical image, ground-based radar, and SAR images [1]. In the case of an optical sensor, the images are generated in a short time while the data of a SAR system is produced in a longer time which reach serval seconds even minutes [2]. Since SAR images can monitor the target in a relative long period of time, it is possible for us to use SAR images to identify moving targets which is well known as Ground Moving Target Identification (GMTI) [3]. On the other hand, SAR is an all-time all-weather senor, regardless of the influence of bad weather and night. Many countries have constructed their own space-borne SAR satellites in the past twenty years [4]. Among them, TerraSAR-X/TanDEM-X SAR satellites, constructed by German Aerospace Center (DLR), have high resolutions and high image quality, which has attracted many attentions in the research field[5].

To obtain the velocity of ships in TerraSAR-X data, there are many methods to deal with SAR image data [6][7]. Most of these methods require extra information or demand special configurations, which make the traditional method narrow for applications [8]. Little attention has been focused on the kinetic information contained in the SAR product itself [9]. In this paper, we realize the extraction task by measuring the defocusing effect of SAR images.

This paper is organized as follows. First, the SAR signal model of moving target was analyzed, and the defocused effect is discussed in Section 2. In section 3, an autofocus method to the image patches of moving targets is proposed and the relationship between phase errors caused the defused effect and the azimuth velocity is revealed. AIS data is used to validate the proposed method and the experimental results are shown in Section 4. Finally, conclusions are drawn in Section 5.

2 Moving target signal model

We briefly review the signal model of moving targets in Section 2.1 and deduct how the model affect the final SAR images in Section 2.2. In this paper, it is assumed that the SAR system operating in strip map mode and the squint angle being zero for all the following derivations.

2.1 Basic SAR signal model

A range-compressed azimuth signal received by the SAR devices, which is demodulated to the baseband for simplifying the signal processing, can be modelled as [10]

$$s(t) = A(t)\,rect\left[\frac{t-t_{bc}}{T_{SA}}\right]\exp\left\{j\frac{4\pi}{\lambda}r(t)\right\} \qquad (1)$$

where $A(t)$ contains the two-way azimuth antenna pattern, the target reflectivity, and propagation losses; t_{bc} is the beam center time; and T_{SA} denotes the synthetic aperture time. The rectangular function *rect*[.] is used for pointing out that the azimuth signal is centered around t_{bc} and that its duration is practically limited by T_{SA}. Focusing on the exponential term, the part in (1) can be written as:

$$\begin{aligned} S(t) &= \exp\left\{-j\frac{4\pi r(t)}{\lambda}\right\} \\ &= \exp\left\{j\left[2\pi f_{dc}(t-t_{bc}) + \pi f_{dr}(t-t_{bc})^2\right]\right\}\exp\left(-j\frac{4\pi r_{bc}}{\lambda}\right) \end{aligned} \qquad (2)$$

where

$$f_{dc} = -\frac{2}{\lambda} v_{r0}$$
$$f_{dr} = -\frac{2}{\lambda}\left(\frac{v_e^2 - 2v_{x0}v_p}{r_{bc}} + a_r\right). \quad (3)$$

v_r, v_x and a_r are the range direction velocity, the azimuth direction velocity and the range direction acceleration of a target, respectively, and v_p is the velocity of the radar platform which moves along the azimuth direction. f_{dc} is called the Doppler centre frequency and f_{dr} is called the Doppler rate. For the details, we refer to [10]. Having (3), it is possible to relate the kinetic parameters with the signal the SAR recorded. The format of (3) is "chirp" which has a second-order term in the exponential component. Based on the signal model, we use the searching method to find the real f_{dr} of the target and then recover the azimuthal velocities.

2.2 Defocusing effect caused by the target movement

After range compression, the main goal is to focus the data in the azimuth direction. The matched filter method usually completes this step [11], which can detect the signal which is most like to the desired signal. As for a chirp signal, the output of the matched filter is a sinc function which is called the point spread function in SAR. It is the basic unit of SAR images and is an important function to evaluate the SAR images. To generate a good SAR image, one of the most important steps is choosing an appropriate signal in the azimuth compression. But how to select the best one is still a challenge. Ordinarily, most of the targets in the scene are stationary, which means the perfect signal inputted in the matched filter has the same parameters. However, when the target becomes moving, using the former designed parameters, the final image cannot reach the best.

In SAR imaging, this kind of phenomena is called "defocusing". In this part, we want to show why the matched filter fails to image the moving target mathematically. In linguistic works, it is because the "designed" signal is no longer equal to the "desired" signal moving target. To specify the mismatch, the mathematic theory is established to analysis the behavior of moving targets. Because the azimuth signal is a chirp signal, we first analyze the mismatched situation. The chirp signal of a moving target can be expressed as follows:

$$s(t) = \exp\left\{j\left[2\pi f_{dc}(t - t_{bc}) + \pi f_{dr}(t - t_{bc})^2\right]\right\} \quad (4)$$

For the sake of convenience, the chirp signal should be transformed into frequency domain where the matched filter processing has a simple representation. According to the theory of stationary phase [12], the amplitude and phase of $S(\omega)$ can be written as:

$$|S(\omega)| = \frac{1}{\sqrt{f_{dr}}} rect\left(\frac{\omega - 2\pi f_{dc}}{2\pi f_{dr} T_{SA}}\right) \quad (5)$$

$$\Phi(\omega) = -\omega t_k + \varphi(t_k) + \frac{\pi}{4} = -\frac{\omega^2}{4\pi f_{dr}} + \frac{f_{dc}\omega}{f_{dr}} - \frac{\pi f_{dc}^2}{f_{dr}} + \frac{\pi}{4} \quad (6)$$

In the above formulas, the amplitude of $S(\omega)$ is a window function and the phase is a quadratic function. To eliminate the second-order terms the matched filter is applied by multiplying the conjugation of $S(\omega)$. Thus, the output of the matched filter becomes a rectangle window function which corresponds to a sinc function in the time domain.

(5) and (6) are the "desired" signal model for general cases. When the target is stationary, $f_{dc} = 0$ and $f_{dr} = 2v_p^2/\lambda r_{bc}$, which is the common situation. When the target is moving, which is defined by (v_{x0}, v_{r0}, a_r), f_{dc} and f_{dr} of the "desired" signal become different. When v_{r0} has value and the two others are zeros, f_{dc} changes and the linear phase in $\Phi(\omega)$ still exists. As a result, the final image will have a displacement with respect to its real position. The other situation is v_{x0} or a_{r0} has value, f_{dr} changes. In this case, if we still use the parameters for stationary targets, the second-order term remains, and the output becomes another kind of chirp signal whose presentation in the time domain is a defocusing sinc function. Hereto, we analyze the influence of (v_{x0}, v_{r0}, a_r) on the representation of the SAR image seen by human eyes.

In the next section, we proposed an autofocus algorithm to refocus the affected SAR images. Meanwhile, the azimuthal velocities can be recovered as a product of the proposed autofocus method.

3 SAR autofocus based on minimum entropy criterion

Movements make images defocused while autofocus algorithms make the images clear again. There are many autofocus algorithms to remove the influence of station instability, errors and so on [13]. The pixel value after the autofocus processing can be formulated as [14]

$$s_l(n) = \frac{1}{N}\sum_{k=0}^{N-1} S_l(k) \exp\{j\varphi_k\} \exp\left\{j\frac{2\pi}{N}kn\right\} \quad (7)$$

where l is the indictor in range direction, n is the indictor in azimuth direction, N is the azimuth sample number and $S_l(k)$ represents the azimuth Fourier transform of the selected lth dominant scattered data after range compression, range migration correction, and rough azimuth compression. The indices k refers to the azimuth frequency, respectively, and φ_k is utilized to cancel phase errors. Hereto, we have obtained the basic formula of autofocus methods whose goal is to find the proper φ_k based on different criteria.

3.1 Minimum-Entropy Criterion

Information entropy is defined as the average amount of information produced by a probabilistic stochastic source of data. As for SAR images, the high entropy means there are many changes and noise in pixel values. The SAR images which are better focused have smaller entropy. Therefore, SAR image autofocus is performed by satisfying the global minimum-entropy criterion to find φ_k. The image entropy is defined as

$$E = -\frac{1}{C}\sum_{l=1}^{L-1}\sum_{n=0}^{N-1}\left|s_l(n)\right|^2 \ln\left|s_l(n)\right|^2 + \ln C \tag{8}$$

where

$$C = \sum_{l=1}^{L-1}\sum_{n=0}^{N-1}\left|s_l(n)\right|^2 \tag{9}$$

The entropy is a conception in information theory which dedicate the minimum bit to encode a message. The extension to the SAR image autofocus domain is quite reasonable because it forces the SAR image use minimum pixel values to represent the same targets. With this criterion, the extent of SAR defocusing is defined in a mathematical way. Thus, it is possible to find a connection between SAR image data and the moving parameters.

3.2 Processing in TerraSAR-X data

The phase error in the range-Doppler domain caused by azimuth velocity is

$$\varphi_k = \frac{\Delta f_{dr}}{\left(f_{dr}^* + \Delta f_{dr}\right) f_{dr}^*}\frac{\omega_k^2}{4\pi} \tag{10}$$

where

$$\Delta f_{dr} = \frac{4 v_{x0} v_p}{\lambda r_{bc}} - \frac{2 a_r}{\lambda} \tag{11}$$

and f_{dr}^* is the Doppler rate used for stationary targets., a_r is generally negligible. Thus, the velocity estimation based on the minimum-entropy criterion can be written as

$$v_{x0} = \arg\min_{v_{x0}\in[v_1,v_2]} E\left(s_l(n); \varphi_k(v_{x0})\right) \tag{12}$$

For the processing of TerraSAR-X data, the proposed method is processed as follows:

1. Determinate the position of the ship and select the region of interest to reduce the data amount.
2. Calculate the f_{dr}^* used for focusing in the XML file.
3. Design a region of $\Delta f_{dr} \in \left[\Delta f_{dr}(v_1), \Delta f_{dr}(v_2)\right]$ that caused by the ship motion.
4. Get the compensate phase obtained by the formula (11)
5. Transfer the processed image to the Range-Doppler domain.
6. Compensate the phase using the result in step 4 and processed in the Range-Doppler domain.
7. For every Δf_{dr} , the refocused images are stored to calculate their entropy.
8. After getting Δf_{dr} which accord to the minimum-entropy, the velocity in azimuth direct can be obtained as follows:

$$v_{x0} = \frac{\lambda \Delta f_{dr} r_{bc}}{4 v_p} \tag{13}$$

4 Experiment results

In order to verify the validity of the proposed method, TerraSAR-X SAR images have been analysed to compare the velocity extracted from SAR images with real data. For the convenient of data acquisition, the Strait of Gibraltar has been chosen as test site which has plenty of ships. The parameters of the TerraSAR -X satellite are given in Table 1, the experiments are conducted by processing several ships.

Table 1 Parameters of TerraSAR -X images

Platform velocity	v_p	7687 m/s
Synthetic aperture time	T_{SA}	0.4063 s
Wavelength	λ	0.0311 m
Azimuth spacing	$S_{azimuth}$	1.9872 m
Range spacing	S_{range}	0.9094 m
Pulse Repetition Frequency	PRF	3562 Hz
Slant range distance	r_{bc}	615000 m

We have chosen two ships to exhibit the ability of our method. The experiment on Ship 1 is shown in Figure 1. The original image is directly for the TerraSAR-X SLC (Single Look Complex) data, the refocused image is processed by the entropy method with the minimum-entropy. The curve figure is the searching results. As can be seen

from Figure 1(c), the minimum-entropy stands at the point -20, which means the azimuth velocity can be estimated as:

$$v_{x0} = \frac{\lambda(-20) r_{bc}}{4 v_p} = -13.026\, m/s \qquad (14)$$

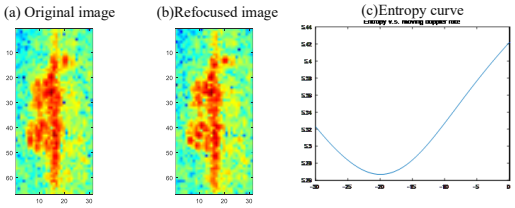

Figure 1: Experiment results of ship 1 (a) original image (b) refocused image (c) entropy cure.

We regard the tail of the ship as a qualitative indicator to validate whether it is moving or not. The tails of the moving ship are shown in Figure 2.

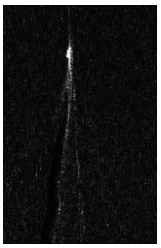

Figure 2: The tails of ship 1 on the sea.

In Figure 2, we can see the track of the ship which validate it is moving. Besides, the track is heading toward to the upper, which confirms that the Δf_{dr} caused by azimuth velocity is negative. The second experiment is conducted on a stationary ship. The experimental results are shown in Figure 3. In Figure 3(c), the minimum-entropy locates in the zero point, where $\Delta f_{dr} = 0$. In other words, the ship is anchored. It can be predicted by checking the tails of the ship in Figure 4.

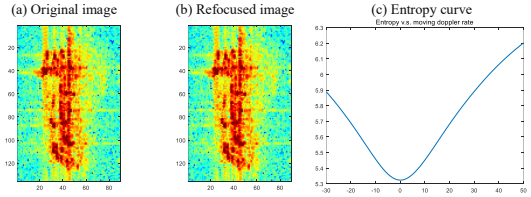

Figure 3: Experiment results of ship 2 (a) original image (b) refocused image (c) entropy cure.

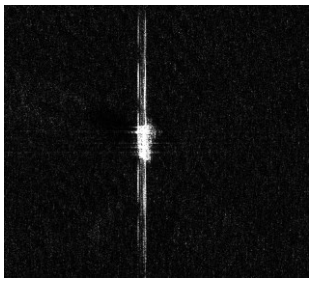

Figure 4: The tails of ship 2 on the sea.

5 Conclusions

In this paper, we proposed a moving ship velocity estimation method based on minimum-entropy criterion. in our method, only the azimuthal velocity is detectable, and the radical velocity is immeasurable. The entropy-based method searches the phase errors according to the SAR signal model of moving targets. Through finding the phase error corresponding to the minimum-entropy, in which the image patches of moving targets are autofocused well, the velocities are obtained. The experiment proves that the moving ship velocity estimation based on minimum-entropy criterion reaches a good performance. In further research, we will refine the experiment on TerraSAR-X data and find methods to extract the velocity component in the range direction.

References

[1] D.Y. Ao, Y.H. Li, C. Hu, and W.M. Tian, *Accurate Analysis of Target Characteristic in Bistatic SAR Images: A Dihedral Corner Reflectors Case*, Sensors, vol.1, no. 18, p. 24, 2018.

[2] Y.H. Li, A. Monti Guarnieri, C. Hu, and F. Rocca, *Performance and Requirements of GEO SAR Systems in the Presence of Radio Frequency Interferences*, Remote Sens., vol. 1, no.10, p. 82, 2018.

[3] Dongyang Ao, Mihai Datcu, *Moving Ship Velocity Estimation Using TanDEM-X Data Based on Sub-Aperture Decomposition*, IEEE Geoscience and Remote Sensing Letters, under reviewing.

[4] Zeng T, Ao D, Hu C, et al. *Multiangle BSAR imaging based on BeiDou-2 navigation satellite system: Experiments and preliminary results* ', IEEE Transactions on Geoscience and Remote Sensing, 53, (10), pp. 5760-5773, 2015.

[5] G. Krieger, A. Moreira, H. Fiedler, I. Hajnsek, M. Werner, M. Younis, et al., *TanDEM-X: A satellite formation for high-resolution SAR interferometry,* IEEE Transactions on Geoscience and Remote Sensing, vol. 45, pp. 3317-3341, 2007.

[6] C. H. Gierull, *Statistical analysis of multilook SAR interferograms for CFAR detection of ground moving targets,* IEEE Transactions on Geoscience and Remote Sensing, vol. 42, pp. 691-701, 2004.

[7] S. Hinz, F. Meyer, M. Eineder, and R. Bamler. *Traffic monitoring with spaceborne SAR—Theory, simulations, and experiments,* Comput-er Vision and Image Understanding, vol. 106, pp. 231-244, 2007.

[8] C. H. Gierull, D. Cerutti-Maori, J. H. G. Ender. *Ground moving target indication with tandem satellite constellations,* IEEE Geoscience and Remote Sensing Letters, vol. 5, no. 4, pp. 710-714, 2008.

[9] G. Lv, J. Wang, and X. Liu, *Ground moving target indication in SAR images by symmetric de-focusing*, IEEE Geoscience and Remote Sensing Letters, vol. 10, pp. 241-245, 2013.

[10] S. V. Baumgartner and G. Krieger, *Dual-Platform Large Along-Track Baseline GMTI,* IEEE Transactions on Geoscience and Remote Sensing, vol. 54, pp. 1554-1574, 2016.

[11] Ao D, Wang R, Hu C, et al. *A Sparse SAR Imaging Method Based on Multiple Measurement Vectors Model*, Remote Sensing, vol. 9, no. 3, p. 297, 2017.

[12] Gierull, C.H., Sikaneta, I.C., Cerutti-Maori, D., *Space-based SAR-Ground Moving Target Indication, Chapter II.7 in Novel Radar Techniques and Applications*, Co-Eds., R. Klemm, U. Nickel, C.H. Gierull, H. Griffiths, P. Lombardo, W. Koch, IET Publishers, London, UK, 2017

[13] X. Li, G. Liu, and J. Ni, *Autofocusing of ISAR images based on entropy minimization*, IEEE Trans. Aerosp. Electron. Syst., vol. 35, no. 4, pp. 1240–1252, Oct. 1999.

[14] T. Zeng, R. Wang, and F. Li, *SAR image autofocus utilizing minimum-entropy criterion,* IEEE Geoscience and Remote Sensing Letters, vol. 10, pp. 1552-1556, 2013.